PAPER

Check for updates

High comprehensive properties of colorless transparent polyimide films derived from fluorine-containing and ether-containing dianhydride†

Yan Shi,‡[a] Jinzhi Hu,‡[a] Xiaomin Li, [iD] [ab] Jing Jian,[a] Lili Jiang,[a] Chuanqiang Yin, [iD] *[ab] Yuchun Xi,[b] Kai Huang,[a] Liejun Su[a] and Lang Zhou[ab]

Fluorinated colorless transparent polyimide (CPI) films are crucial for flexible displays and wearable devices, but their development is limited by high costs and relatively low mechanical properties. In this study, a series of colorless transparent polyimide films was synthesized by incorporating the cost-effective ether-containing diamine, 4,4′-isopropylidenediphenoxy bis(phthalic anhydride) (BPADA), into commercially available 4,4′-(hexafluoroisopropyl)diphthalic anhydride (6FDA) and 2,2′-bis(trifluoromethyl)benzidine (TFMB). The comprehensive properties of the films were systematically investigated using a combination of experimental and numerical methods, including molecular dynamics (MD) simulations and density functional theory (DFT). This study focuses on exploring the influence of varying dianhydride ratios on the aforementioned properties. The incorporation of BPADA in the dianhydride significantly enhances the mechanical properties and flexibility of the film. When the ratio of ether anhydride to fluorine anhydride is 4 : 6 (CPI-4), the tensile strength is 135.3 MPa, and the elongation at break is 8.3%, which is 109.6% and 118.45% higher than that of the original film without ether anhydride. This research provides valuable insights for the future application of new polyimide materials in flexible display devices.

1. Introduction

Polyimide plays a significant role in various important fields such as foldable mobile phones, flexible wearable devices, 5G technology and other optoelectronic devices due to its exceptional performance.[1–4] In recent decades, as technological advancements have raised performance requirements, transparent polyimides have garnered attention in flexible display technology and wearable devices.[5–9] Flexible display materials require strong light transmittance, high temperature resistance and foldability.[10,11] However, traditional polyimides typically exhibit a yellowish-brown color with poor transparency, making them unsuitable for use in optoelectronics due to the presence of charge transfer complexes (CTCs) within or between molecular chains.[5] In order to solve this problem, the CTCs effect must be suppressed. A common strategy is to adjust and change the molecular structure of polyimide with dianhydrides and diamine monomers. This can be achieved through the incorporation of special groups, such as trifluoromethyl,[12–14] alicyclic structure,[9,15,16] non-planar

structure,[17,18] and large volume side groups.[19–22] However, challenges still exist in addressing the transparency and thermal properties of polyimide films. For instance, the introduction of non-planar structures may result in molecular chain disorder and increase free volume, thereby reducing the CTC effect and enhancing film transparency. However, this will eventually affect the thermal resistance of the film. Additionally, the addition of a large volume of side groups can increase the free volume and improve transparency, but also lead to decrease in the yellowness of the film.

Fluorine groups, are well-known for their strong electron-withdrawing ability and large free volume, which can effectively weaken the charge transfer (CT) effect and enhance transparency. Therefore, adding fluorine atoms to the polyimide molecular chain is a widely used strategy to improve transparency.[23–25] For example, Liu *et al.*[26] designed and synthesized a fluorinated aromatic diamine monomer, 3,3′-diisopropyl-4,4′-diaminodiphenylmethane-4″-trifluoromethyl-methane (PAPFT), and polymerized it with various commercial dianhydrides to produce highly heat-resistant and transparent PI films. These films exhibited a cutoff wavelength ranging from 307 to 362 nm, with a transmittance exceeding 86% in the visible light range. The glass transition temperature (T_g) ranged from 261 to 331 °C, the dielectric constant at 1 MHz ranged from 2.75 to 3.10, and the contact angle ranged from 87.3° to 93.9°. However, they still suffered from poor mechanical properties. Specifically, the film fabricated from PAPFT and 4,4′-

[a]*Institute of Photovoltaics, Nanchang University, Nanchang 330031, P. R. China. E-mail: cqyin@ncu.edu.cn*

[b]*Institute of New Materials Technology, NCU-GQC Institute of PV-HE-ES Technology, Jiujiang 332020, P. R. China*

‡ These two authors contributed equally to this paper.

(hexafluoroisopropylidene)diphthalic anhydride (6FDA) exhibited a tensile strength of only 69.4 MPa and a Young's modulus of 1.7 GPa. Such inferior mechanical performance severely limited its application in the field of flexible displays. Nevertheless, this approach remains one of the most widely researched and commercially mature types of thin film materials in academia. In the process of polyimide preparation, copolymers containing flexible groups such as ether bonds can increase flexibility and improve film formation.[27] Generally, PI molecules possess high rigidity and partial crystallinity, making them difficult to dissolve.[28–30] However, the addition of BPADA helps to reduce the viscosity and increase the solubility of polyamic acid (PAA).[31–34] J. H. Chang et al.[35] synthesized CPI films with BPADA and three diamines of different structures and applied them to flexible display panels. The PI films synthesized by BPADA and bis(3-aminophenyl)sulfone (APS) exhibites a high transmittance of 98% at a wavelength of 550 nm. In addition, all films demonstrated excellent solubility in common solvents such as chloroform, dichloromethane, N,N'-dimethylacetamide, and pyridine. In addition, some researchers have successfully introduced BPADA into PI to prepare low dielectric constant films. For instance, PI consisting of BPADA and 2,2-bis(4-(4-aminephenoxy)phenyl)propane (BAPP) demonstrated a dielectric constant of 2.32.[36]

In this study, we aimed to enhance the comprehensive performance and reduce the manufacturing cost of traditional fluorinated polyimides by synthesizing a series of transparent polyimides. To achieve this, we combined the cost-effective dianhydride BPADA with 6FDA and 2,2'-bis(trifluoromethyl) biphenylamine (TFMB). Colorless polyimide (CPI) films with excellent properties were prepared by two-step copolymerization. The optical and thermal properties of the copolymer were studied systematically, varying the proportions of ether bonds and fluorinated groups. Molecular dynamics (MD) simulation was utilized to analyze the conformation and free volume fraction of the polymer. Additionally, the optical properties of the polymers were analyzed using density functional theory (DFT). All the CPI films exhibited certain transparency, higher decomposition temperature for thermal resistance, and lower dielectric parameters. Using a balance component of 6FDA and BPADA, the film with excellent comprehensive properties was obtained by adjusting the molecular design of the dianhydride ratio. The addition of 6FDA improved the heat resistance of the film, while the addition of BPADA improved the mechanical properties of the film. Thus, this work provides a practical approach for developing high-performance colorless polyimide films.

2. Experimental section

2.1 Materials

4,4'-(Hexafluoroisopropylidene)bisphthalic anhydride (6FDA, 99.5%), 2,2'-bis(trifluoromethyl)benzidine (TFMB, 99.5%) and 4,4'-(4,4'-isopropylidenediphenoxy)bis (phthalic anhydride) (BPADA, 99.5%) were purchased from Zhongtai Chemical (Tianjin) Co., Ltd (China). N,N'-Dimethylacetamide (DMAc, AR) was supplied by Sinopharm Chemical Reagent Co., Ltd (China).

All materials were used according to the supplied standards without additional purification.

2.2 Synthesis and preparation of polyimide films

This experiment employed a two-step method (Fig. 1) to fabricate CPI films. Although the synthesis routes for all CPI films with different dianhydride ratios were nearly identical, only the synthesis process of CPI-3 film is described here (Table 1 provides the different molar ratios of diamine to dianhydride and their corresponding abbreviation in the study). First of all, TFMB (18.5 mmol, 5.9286 g) was dissolved in 45 g DMAc solvent and stirred for 30 minutes to dissolve the diamine. Then, BPADA (11.1 mmol, 5.7817 g) and 6FDA (7.4 mmol, 3.2898 g) were added to the above solution. The molar ratio of diamine TFMB to dianhydrides BPADA and 6FDA was 10 : 6 : 4, and the solid content was adjusted to 25%. The mixture solution was stirred in a cold bath at 5 °C for 24 hours to form a colorless and transparent polyamide acid solution. Next, the as-prepared solution was applied onto a clean glass plate, and an even coating process of the film was achieved using a scraper. Subsequently, the film was placed in an oven and heated at 60 °C for 1 hour. Afterward, the dried film was removed and clamped into the furnace for the gradient heating process (150 °C/1 hour, 210 °C/0.5 hour, 240 °C/0.5 hour, 270 °C/1.5 hours). Finally, a transparent, colorless and flexible CPI film was obtained, as shown in Fig. 1.

2.3 Characterization

The chemical structure of the PI film was determined using a Fourier transform infrared spectrometer (FT-IR, iS50, Thermo Fisher Scientific, Inc). The aggregation state of the PI films was characterized by X-ray diffraction (XRD, D8 Discover, Bruker, Germany). The molecular weights were tested by a gel permeation chromatography (GPC E2695, Waters Alliance, SG) system equipped and a Sepax high-resolution chromatography column using DMAc as the eluent, and the system was calibrated with monodisperse polystyrene standards. The glass transition temperatures of the films were measured dynamic thermomechanical analyzer (DMA 242E, Netzsch, Germany) and differential scanning calorimeter (DSC 214, Netzsch, Germany), respectively. The thermal expansion coefficient of the film was determined using a static thermomechanical analyzer (TMA 402F3, Netzsch, Germany). The thermalgravimetric weight losses of the films were measured using a simultaneous thermogravimetric analyzer (STA 2500, Netzsch, Germany). The color coordinates of the film were determined using a color haze meter (3nh YS6002, China), following CIE (International Commission de I'Eclairage) standards and D65 illumination. The ultraviolet-visible (UV-Vis) spectrum was obtained using a spectrophotometer (Lambda750S, PerkinElmer, America). Dielectric properties were evaluated using impedance analyzer (E4990A, Keysight, America) at frequencies ranging from 10 MHz to 1000 Hz.

2.4 Simulation details

With the advancement of science and technology, molecular dynamics simulation has gained substantial attention and
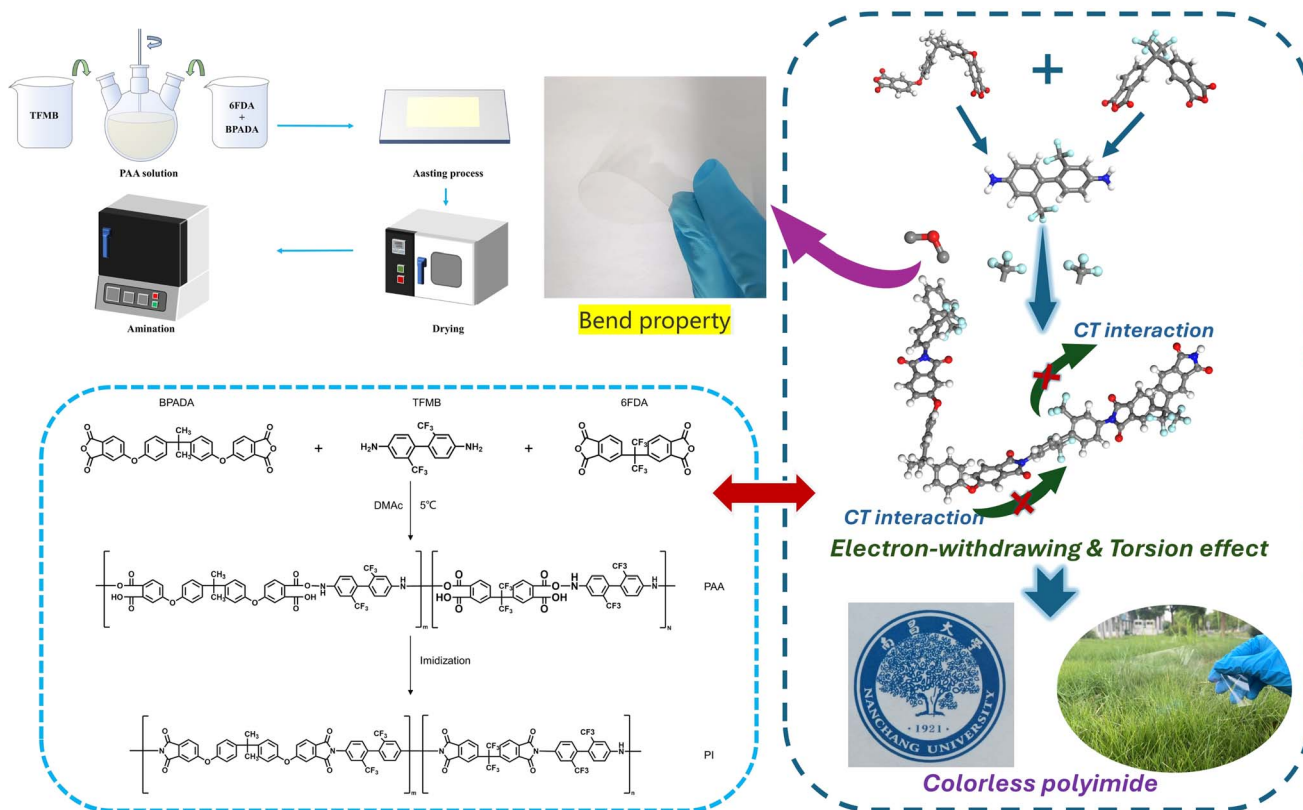
Fig. 1 Synthesis procedure for polyimides.

Table 1 Proportion of fluorine-containing dianhydride and ether-containing dianhydride components and GPC data for CPIs

Number	n(BPADA) : n(6FDA) : n(TFMB)	GPC data		
		$M_w \times 10^4$	$M_n \times 10^4$	M_w/M_n (PDI)
CPI-1	10 : 0 : 10	5.32	3.26	1.63
CPI-2	8 : 2 : 10	5.84	3.47	1.68
CPI-3	6 : 4 : 10	6.53	3.81	1.71
CPI-4	4 : 6 : 10	7.20	3.90	1.85
CPI-5	2 : 8 : 10	7.94	3.95	2.01
CPI-6	0 : 10 : 10	8.20	4.70	1.74

development, making it a widely utilized approach in the field of materials.[37–39] Molecular dynamics simulation allows for a comprehensive exploration of the properties and structures of polyimides from various angles, including molecular chain configuration and size.[40,41] In this study, six amorphous models were created using the Material Studio (MS) software package. The COMPASS force fields were employed for spatial geometric optimization and dynamic optimization, while the Forcite module facilitated the completion of the dynamic equilibrium process.

The relationship between the structure and properties of PI films was evaluated through the determination of molecular orbital energy.[42] In order to optimize the geometric structure of PI, the Gaussian 09 program was employed using density functional theory (DFT) method. This allowed for the calculation of various molecular orbitals including the highest

occupied molecular orbital (HUMO), the lowest unoccupied molecular orbital (LUMO), and the band gap (E_{GAP}, calculated as the difference between E_{HUMO} and E_{LUMO}). The calculation of these properties was conducted using the B3LYP method at the theory level and the 6-31g(d) basis set.

3. Results and discussion

3.1 Chemical structure characterization of CPI films

A series of CPI films were synthesized *via* a two-step procedure to incorporate fluorine functional groups. Fourier infrared spectroscopy results demonstrate that the functional groups measured corresponded to the molecular structure of polyimide, as shown in Fig. 2a. FTIR spectra shows that the characteristic absorption peaks of the polyimide ring at 1787 cm^{-1} and 1730 cm^{-1} are symmetric C=O stretch and asymmetric
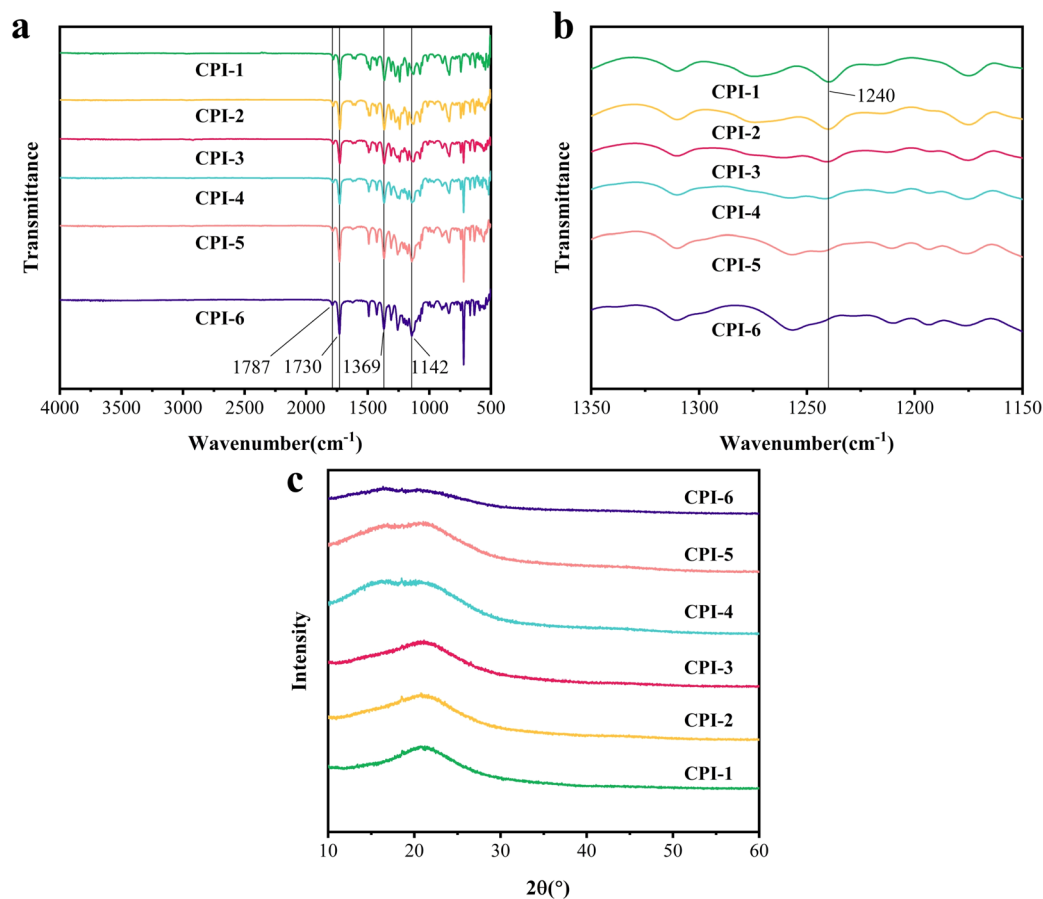
Fig. 2 Chemical structure characterization of the as-obtained CPI films: (a and b) FTIR spectrum, (c) XRD patterns.
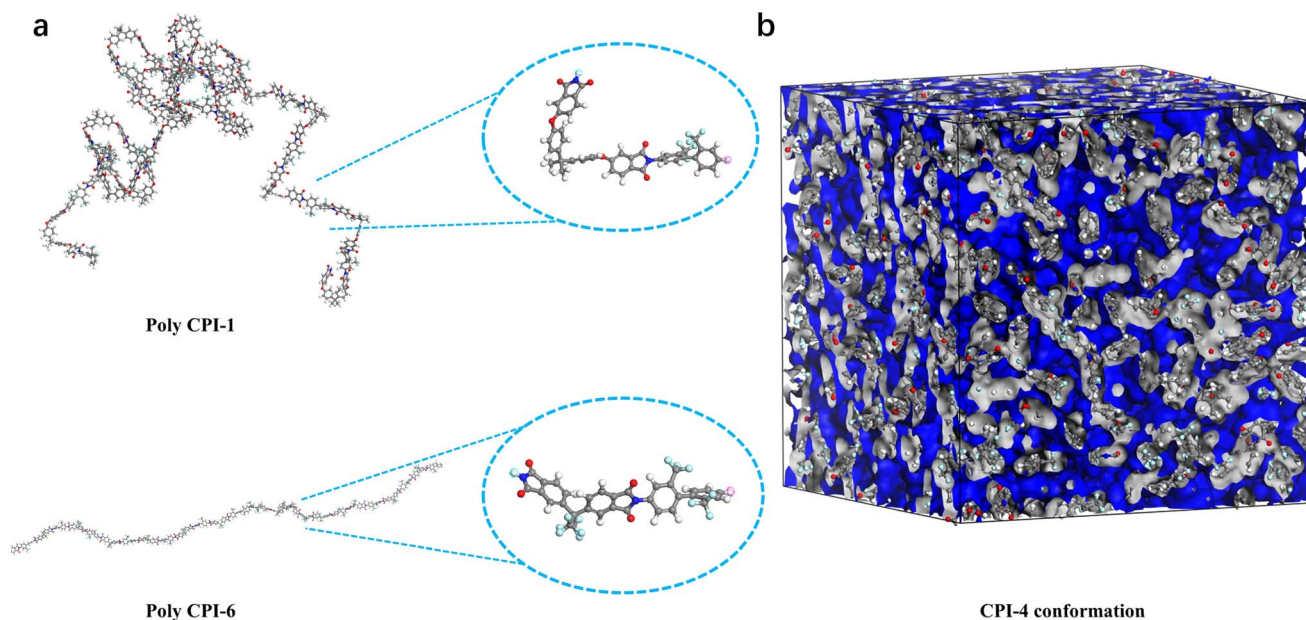

Fig. 3 (a) The molecular chain conformation and repeat unit conformation after structural optimization (C: grey, H: white, O: red, N: blue, F: cyan); (b) fraction free volumes (FFV) of polyimides.

C=O stretch, respectively, while the absorption peak near 1369 cm^{-1} corresponds to the C–N stretching vibration. Fluorine-containing groups can be corroborated by observing an absorption peak that indicates C–F stretching vibrations, typically appearing around 1142 cm^{-1}, which absorption intensity exhibits a positive correlation with the augmented

6FDA content. Fig. 2b illustrates the absorption peak of an irregular stretching vibration associated with the ether bond, typically manifesting around 1240 cm^{-1}. Notably, the absorption strength decreases proportionally with the reduction of BPADA content. In addition, there are no characteristic peaks of polyamic acid near 1500 cm^{-1} and 3200 cm^{-1}, indicating that the synthesized films are completely imidated.

The condensed structures of the as-obtained CPI films were characterized by XRD analysis. As shown in Fig. 2c, the amorphous diffuse scattering was observed within the range of $2\theta = 16°$ to 21°. The peak exhibited a broad diffraction profile with low intensity, which is characteristic of polyimide. The average molecular chain spacing d of the polyimide film was determined[12] and is presented in Table S1 in the ESI.† It was found that the average molecular chain spacing increased with the number of –CF$_3$ groups, ranging from 4.2494 Å for CPI-1 to 5.4126 Å for CPI-6. This suggests that the stack of molecular chains gradually becomes loose, as the presence of –CF$_3$ leads to greater spatial obstruction, disrupting the regularity of the molecular chain and increasing the free volume. It is noteworthy that the presence of flexible ether bonds facilitates the stacking of the entire molecular chain. Table 1 also lists the GPC data for the CPIs, and these polymers possess high molecular weight, with M_w in the range of 5.32–8.2 × 10^4 g mol^{-1}, M_n in the range of 3.26–4.7 × 10^4 mol^{-1}, and the polydispersity index (M_w/M_n) at 1.63–2.01.

To explore the relationship in polyimide molecular structures, we conducted molecular dynamics (MD) simulation calculations to analyze the molecular conformation and fraction free volume (FFV) of polyimide. The optimized structure is depicted in Fig. 3, with number of repeating units of polyimide being 20. It is observed that compared with 6FDA, BPADA exhibits a larger amorphous molecular chain coil and more distorted conformation. As the –CF$_3$ group is gradually introduced, the molecular chain becomes increasingly rigid. Moreover, the bond angles of the ether bonds result in a helical chain structure, creating a large gap for a single molecular chain. Nevertheless, multiple molecular chains intertwine and fill the gaps of each other, resulting in a higher density and lower FFV, as illustrated in Table S1.† As the 6FDA content increases, the overall rigidity enhances, leading to an increased average molecular chain spacing and FFV. This observation aligns well with XRD results, reinforcing the accuracy of our theoretical model.

3.2 Thermal properties

Good heat resistance is essential for the application of CPI materials in the field of optoelectronics.[43] A series of tests were
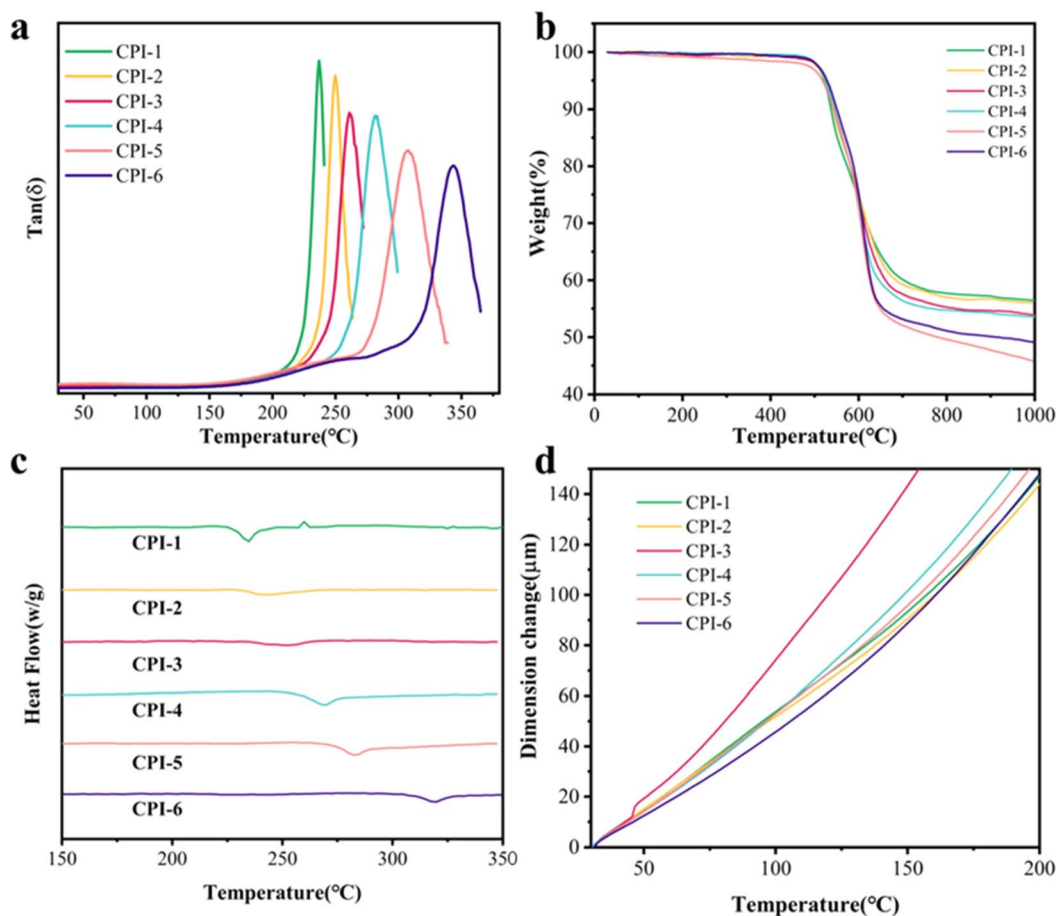

Fig. 4 Thermal properties of CPI films: (a) tan δ curves from DMA, (b) TGA curves, (c) DSC curves, and (d) TMA curves.

Table 2 Thermal and mechanical properties data of CPI films

Number	T_g^a (°C)	T_g^b (°C)	T_5^c (°C)	T_{10}^c (°C)	R_w^d (%)	CTE (ppm K^{-1})
CPI-1	236.8	219.0	521.1	538.5	57.7	58.7
CPI-2	249.7	235.2	521.8	539.3	56.9	57.2
CPI-3	261.4	241.7	524.3	544.3	55.2	67.1
CPI-4	281.7	258.4	524.1	549.1	54.7	61.0
CPI-5	306.4	274.4	515.0	544.9	49.5	62.6
CPI-6	344.2	314.9	526.6	549.0	51.1	60.2

^{a} T_g measured by DMA at a heating rate of 1 °C min^{-1} at 1 Hz. ^{b} T_g measured by DSC at a heating rate of 10 °C min^{-1}. ^{c} The weight loss of 5 wt% and 10 wt%, respectively. ^{d} Residual weight retention at 800 °C under nitrogen atmosphere.

conducted to investigate the influence of different proportions of 6FDA on the thermal properties of PI films. The glass transition temperature (T_g), thermal decomposition temperature (T_d) and thermal expansion coefficient (CTE) of transparent polyimide films were determined through various experiments, including dynamic thermomechanical analysis (DMA), static thermomechanical analysis (TMA), differential scanning calorimetry (DSC) and thermogravimetric analysis (TG). The results of these key parameters are presented in Fig. 4 and Table 2. The presence of a relaxation peak in the DMA curves accurately indicates the glass transition temperature of CPI. The glass transition temperature of CPI series films ranges from 236.8 °C to 344.2 °C (Fig. 4a and Table 2). It was observed that an increase in the number of –CF$_3$ groups led to an increase in T_g. This phenomenon can be attributed to the –CF$_3$ group's obstruction of segmental migration. Specifically, CPI-6, characterized by a higher perfluorinated ratio, exhibited a significantly higher T_g value of 344.2 °C, in contrast to the comparatively lower T_g value of 236.8 °C observed for CPI-1. As shown in Fig. 4b, all series of films exhibited high heat loss temperatures and $T_{d5\%}$ values higher than 510 °C, indicating good thermal processing properties for manufacturing on the production line. Moreover, despite the varying ratios of 6FDA, all polyimide films displayed similar T_5 values, while their T_{10} values slightly increase with increasing 6FDA ratio. Notably, the

residual weight at 800 °C decreased with increasing 6FDA percentage, with CPI-5 having only 49.5% residual weight. The CTE values of these six types of CPI films were all approximately 60 ppm K^{-1}, exhibiting a relatively lower thermal expansion coefficient.

3.3 Optical properties

Good optical transparency is essential for CPI films used in flexible display technology.[44] The optical properties of CPI films, including important factors such as optical transparency (T_{400}, T_{500}, λ_{cutoff}) and color coordinates (L^*, a^*, b^*, YI and haze), were evaluated using UV-Vis spectra and a color haze meter, as shown in Fig. 5 and Table 3. At 400 nm, the optical transmission of all films exceeds 60%. At 500 nm, all films exhibited transmittance levels exceeding 87%, with cutoff wavelengths in the range of 359–378 nm. The presence of a large spatial site resistance of –CF$_3$ in 6FDA, combined with the flexible ether bond in BPADA, facilitates molecular chain stacking. Moreover, as the concentration of 6FDA increases, the free volume also increases, resulting in a weakening of the charge transfer (CT) effect, as indicated by our simulation results. Notably, CPI-4 exhibited remarkably low yellowness and high optical transmittance, as well as an almost colorless appearance (T_{500} = 87.21%, b^* = 1.36, YI = 2.31, and haze = 0.63). Furthermore, to fully understand the optical performance of our work, we

Table 3 Optical properties of CPI films

Number	T_{400}^a (%)	T_{500}^b (%)	λ_{cutoff} (nm)	L^*	a^*	b^*	YI	Haze
CPI-1	63.50	87.17	376	96.21	−0.33	1.67	2.92	0.79
CPI-2	62.96	88.42	378	95.75	−0.36	1.50	2.58	0.56
CPI-3	66.41	88.56	372	95.48	−0.37	1.36	2.31	0.63
CPI-4	65.29	87.21	372	96.29	−0.43	1.58	2.67	1.45
CPI-5	69.95	87.72	366	95.85	−0.40	1.50	2.54	0.71
CPI-6	68.32	87.87	359	96.15	−0.56	1.89	3.15	0.95

^{a} T_{400} means transmittance at a wavelength of 400 nm. ^{b} T_{500} means transmittance at a wavelength of 500 nm.
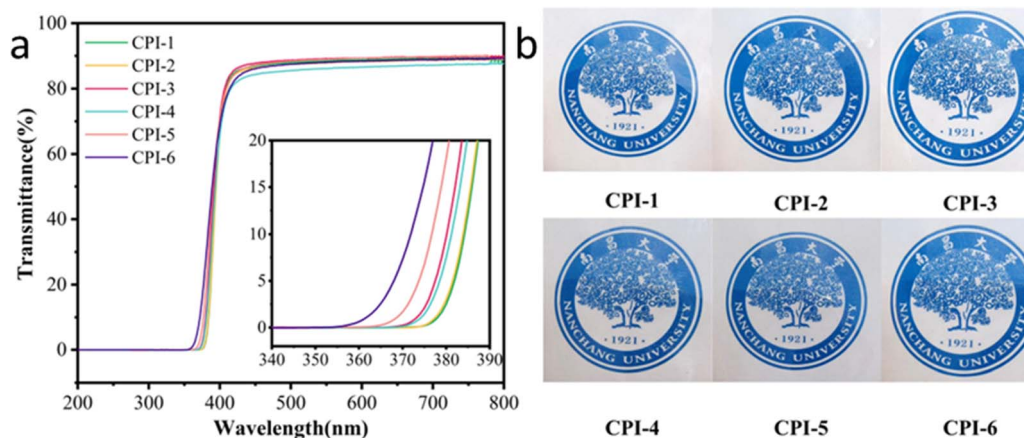

Fig. 5 (a) UV-Vis transmission spectra and (b) visual photographs of CPI films.
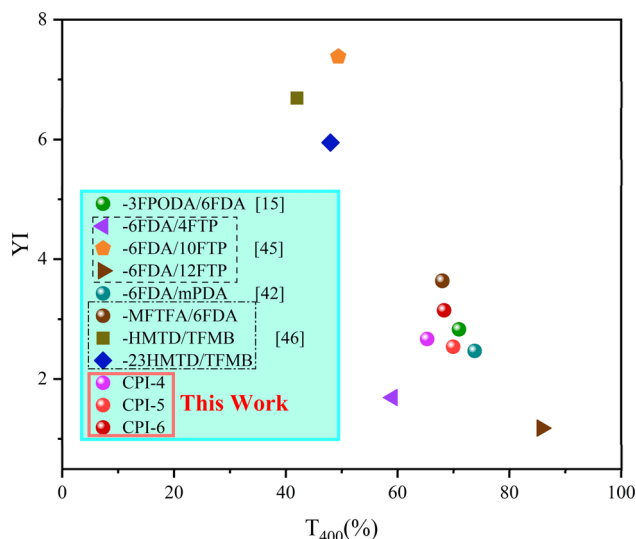
Fig. 6 Comparisons of this work to CPIs reported in the literature.[15,42,45,46]

compare CPI-4, CPI-5 and CPI-6 with CPI reported in recent years. It can be seen that our work has excellent optical performance, as shown in Fig. 6.[15,42,45,46]

To investigate the influence of 6FDA content on the transmittance of PI films, DFT calculations were conducted on four model compounds. The three different polymerization degrees were considered for the molecular chain. The optimized geometric structure and orbital energy results are presented in Fig. 7. Table S2† summarizes the values of the highest occupied molecular orbital energy (E_{HUMO}), lowest occupied molecular orbital energy (E_{LUMO}), energy band gap (E_{GAP}), and the ratio of BPADA and 6FDA in the molecular chain. The energy band gap (E_{GAP}) serves as a measure of the charge transfer (CT) from the

electron-donor diamine to the electron-acceptor dianhydride. A larger E_{GAP} value indicates higher electron excitation energy, which corresponds to a lower cut-off wavelength (λ_{cutoff}) in the UV-visible absorption spectrum and higher optical transmittance.[47,48] Our calculations reveal that an increased proportion of 6FDA leads to a larger energy gap, with CPI-4 having the highest E_{GAP} value due to its perfluorinated ratio. This finding is in good agreement with the experimental results presented in Fig. 5. As the 6FDA content decreases, the cut-off wavelength shifts to wards longer wavelengths. Therefore, it can be concluded that fluorine-containing groups are more effective in inhibiting intramolecular charge transfer compared to ether bonds.

3.4 Dielectric properties and hydrophilicity

The low dielectric constant polyimide film is a crucial parameter for evaluating the potential applications in 5G communications and flexible printing.[49,50] Fig. S1† and 8 illustrate the investigation of the dielectric properties and hydrophilicity of these films. The dielectric constant (ε), dielectric loss (δ), and contact angle to water of the film are shown in Table 4. The dielectric constants of these CPI films range from 2.02 to 2.81. Specifically, the dielectric constant (D_k) at 1 kHz decreases in the following order: CPI-3 (2.81) > CPI-1 (2.75) > CPI-2 (2.57) > CPI-5 (2.37) > CPI-4 (2.30) > CPI-6 (2.02). Generally, the presence of fluorine atoms in 6FDA has a unique electronic effect that reduces the dielectric constant of the film by decreasing its polarizability and increasing its the free volume. As the 6FDA content increases, the contact angle to water on the surface of film increases from 74.1° to 96.4°. This phenomenon can be attributed to the higher electronegativity of the fluorine-containing groups, which enhances the hydrophobicity of the CPI film.
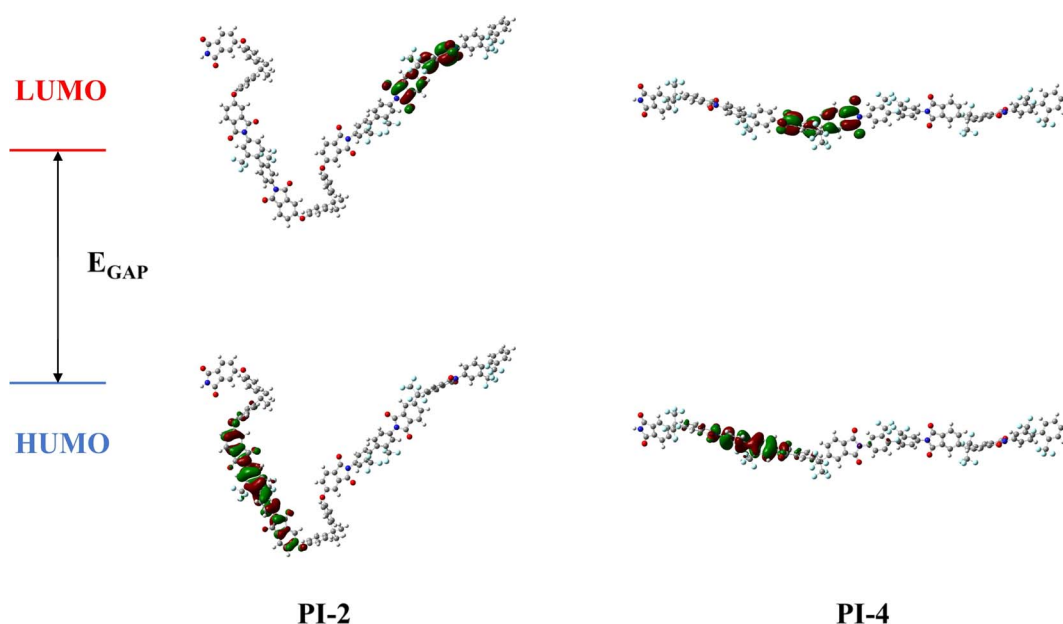

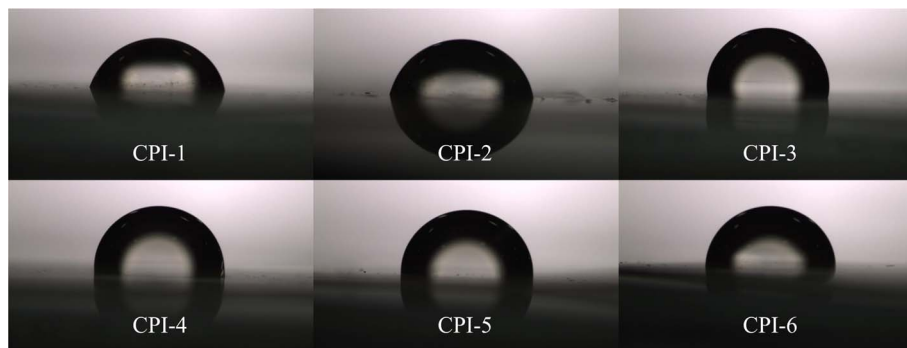**Fig. 7** Molecular orbital (MO) diagrams of the polyimides (C: grey, H: white, O: red, N: blue, F: cyan).

Fig. 8 The contact angle between water and the surface of the CPI film with the variation of the 6FDA content.

Table 4 Dielectric and mechanical properties of CPI films

Number	ε^a	δ^b (10^{-3})	Contact angle (°)	$\sigma_{max}{}^c$ (MPa)	E^d (%)	γ^e (GPa)
CPI-1	2.75	1.42	74.1	87.73	9.6	1.7
CPI-2	2.57	1.46	76.9	100.00	7.9	2
CPI-3	2.81	1.32	82.0	78.86	8.3	1.2
CPI-4	2.30	1.54	86.7	135.19	8.3	1.8
CPI-5	2.37	1.43	91.6	89.07	7.0	1.6
CPI-6	2.02	1.40	96.4	64.54	3.8	2.1

[a] Dielectric constant. [b] Dielectric loss. [c] Tensile strength. [d] Breaking elongation. [e] Elastic modulus.

3.5 Mechanical properties

The robust mechanical property is crucial for the practical application of PI films. The mechanical properties of these CPI films are shown in Fig. 9 and Table 4. The tensile strength ranges from 64.5 MPa to 135.2 MPa, the tensile modulus is between 1.6 GPa and 2.1 GPa, and the elongation at break varies from 3.8% to 9.6%. The presence of BPADA in the PI film contributes to better film-forming properties. However, the preparation process results in increased brittleness due to the rigid structure of 6FDA and TFMB (elongation at break is 3.8%). As the BPADA content in the molecular chain increases, the film's flexibility gradually improves (elongation at break increases from 3.8% to 9.6%). This improvement is attributed to the higher presence of ether bond in BPADA. Notably, when

the ratio of n(BPADA) : n(6FDA) is 4 : 6, the tensile strength reaches 135.2 MPa. Comparing with CPI-6, it is found that even with only 40% of the polymer chain consisting of BPADA, the mechanical properties have increased by 109.6%. The tensile strength increases first and then decreases. This phenomenon may be attributed to two aspects. On the one hand, with the increase of the number of –CF₃ groups, the increase of steric hindrance makes the molecular chain stacking more and more loose, but with the increase of flexible ether bonds, the stacking
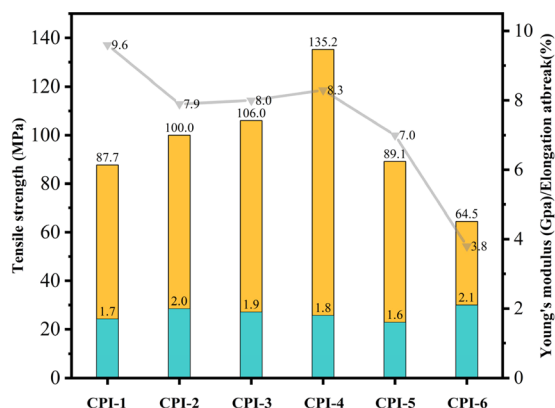

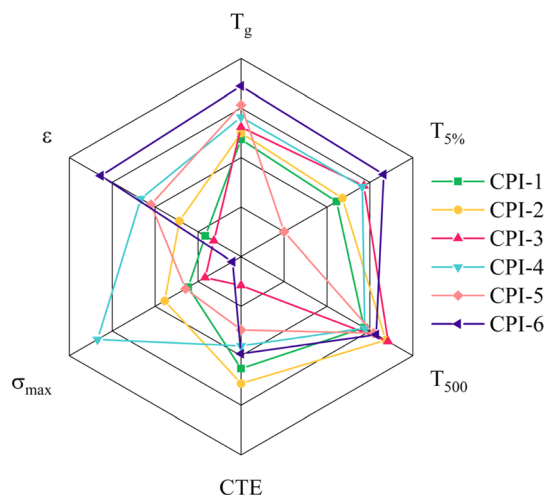Fig. 9 Mechanical properties of CPI films.

Fig. 10 Comparison of key performance parameters among six polyimides: glass transition temperature, T_g; the weight loss of 5 wt%, $T_{5\%}$; optical transmittance at 500 nm, T_{500}; thermal expansion coefficient, CTE; tensile strength, σ_{max}; dielectric property, ε.

and entanglement of the whole molecular chain are promoted, and the tensile strength is gradually improved. On the other hand, the increase of flexible ether bonds enhances the intra-molecular force and hinders the increase of molecular weight during the polymerization process, as shown in Table 1, resulting in a gradual decrease in tensile strength.

In this study, a series of low yellowness and high transparency CPI films were synthesized and their comprehensive performance was investigated. It is evident from Fig. 10 that the CPI-4 film shows the most favorable comprehensive performance among the tested films. This film exhibits high light transmittance, excellent thermal resistance, and impressive mechanical properties. Therefore, it holds great potential for applications in the optoelectronic devices market.

4. Conclusions

In summary, a series of PI films with high transparency, high heat resistance, low dielectric properties, and good mechanical properties have been successfully prepared. The different proportions of fluorine-containing dianhydride 6FDA and ether-containing BPADA were extensively discussed to copolymerize with fluorine-containing diamine TFMB. The effects of fluorine-containing groups and ether bonds on the thermal, mechanical, optical, and dielectric properties of the PI films were systematically investigated. Furthermore, MD and DFT simulations have also quantitatively studied the structure and optical properties of the films. The results showed that the inclusion of 6FDA in the copolymerization increased the spacing between molecular chains and inhibited the formation of charge transfer complexes (CTCs), resulting in improved optical and thermal properties. Additionally, the ether bonds present in BPADA enhanced the film-forming ability and mechanical properties of the PI films, leading to improve the tensile strength and elongation at break. CPI-4 films with T_g of 281 °C, $T_{d10\%}$ of above 540 °C, an optical transmittance of 87.21% at 500 nm, a tensile strength of 135.3 MPa, and an elongation at break of more than 8%. This work offers fundamental insight for achieving a balanced performance in CPI films and highlights the attractiveness of these PI films in flexible optoelectronic applications due to their comprehensive performance. Moreover, their hydrophobicity and low dielectric properties support their potential application in 5G technology.

Data availability

The authors confirm that the data supporting the findings of this study are available within the article and its ESI.†

Conflicts of interest

There are no conflicts to declare.

Acknowledgements

References

1 J. L. Zhang, Y. Y. Sui, J. H. Li, L. Shan, F. F. Niu, G. P. Zhang and R. Sun, Low-dielectric and low-temperature curable fluorinated nano carbon/polyimide composites with 6-aminoquinoline for end capping, *Polym. Compos.*, 2023, **44**(2), 886–896.

2 K. P. Ruan, Y. Q. Guo and J. W. Gu, Liquid Crystalline Polyimide Films with High Intrinsic Thermal Conductivities and Robust Toughness, *Macromolecules*, 2021, **54**(10), 4934–4944.

3 W. Y. Wu, Y. H. Hsu, Y. F. Chen, Y. R. Wu, H. W. Liu, T. Y. Tu, P. Chao, C. S. Tan and R. Horng, Wearable Devices Made of a Wireless Vertical-Type Light-Emitting Diode Package on a Flexible Polyimide Substrate with a Conductive Layer, *ACS Appl. Electron. Mater.*, 2021, **3**(2), 979–987.

4 J. Park, W. Kim, Y. Aggawal, K. Shin, E. Ha Choi and B. Park, Highly Efficient and Stable Organic Light-Emitting Diodes with Inner Passivating Hole-Transfer Interlayers of Poly(amic acid)-Polyimide Copolymer, *Adv. Sci.*, 2022, **9**(9), 12.

5 D. J. Liaw, K. L. Wang, Y. C. Huang, K. R. Lee, J. Y. Lai and C. S. Ha, Advanced polyimide materials: Syntheses, physical properties and applications, *Prog. Polym. Sci.*, 2012, **37**(7), 907–974.

6 L. J. Yang, S. Chi, S. P. Dong, F. Yuan, Z. D. Wang, J. X. Lei, L. X. Bao, J. Xiang and J. L. Wang, Preparation and characterization of a novel piezoelectric nanogenerator based on soluble and meltable copolyimide for harvesting mechanical energy, *Nano Energy*, 2020, **67**, 104220.

7 J. Ren, D. Y. Li, Y. Zhang, W. Z. Yang, H. Y. Nie and Y. Liu, Laser Direct Activation of Polyimide for Selective Electroless Plating of Flexible Conductive Patterns, *ACS Appl. Electron. Mater.*, 2022, **4**(5), 2191–2202.

8 T. Q. Liu, F. Zheng, X. R. Ma, T. M. Ding, S. S. Chen, W. Jiang, S. Y. Zhang Dr and Q. H. Lu, High heat-resistant polyimide films containing quinoxaline moiety for flexible substrate applications, *Polymer*, 2020, **209**, 122963.

9 X. F. Hu, H. L. Mu, Y. X. Wang, Z. Wang and J. L. Yan, Colorless polyimides derived from isomeric dicyclohexyl-tetracarboxylic dianhydrides for optoelectronic applications, *Polymer*, 2018, **134**, 8–19.

10 Z. Y. Zhao, K. Liu, Y. W. Liu, Y. L. Guo and Y. Q. Liu, Intrinsically flexible displays: key materials and devices, *Natl. Sci. Rev.*, 2022, **9**(6), 18.

11 S. D. Kim, B. Lee, T. Byun, I. S. Chung, J. Park, I. Shin, N. Y. Ahn, M. Seo, Y. Lee, Y. Kim, W. Y. Kim, H. Kwon, H. Moon, S. Yoo and S. Y. Kim, Poly(amide-imide) materials for transparent and flexible displays, *Sci. Adv.*, 2018, **4**(10), 10.

12 W. F. Peng, H. Y. Lei, X. X. Zhang, L. H. Qiu and M. J. Huang, Fluorine Substitution Effect on the Material Properties in

Transparent Aromatic Polyimides, *Chin. J. Polym. Sci.*, 2022, **40**(7), 781–788.

13 M. Hasegawa, T. Ishigami, J. Ishii, K. Sugiura and M. Fujii, Solution-processable transparent polyimides with low coefficients of thermal expansion and self-orientation behavior induced by solution casting, *Eur. Polym. J.*, 2013, **49**(11), 3657–3672.

14 H. T. Zuo, F. Gan, J. Dong, P. Zhang, X. Zhao and Q. H. Zhang, Highly Transparent and Colorless Polyimide Film with Low Dielectric Constant by Introducing Meta-substituted Structure and Trifluoromethyl Groups, *Chin. J. Polym. Sci.*, 2021, **39**(4), 455–464.

15 Y. Wang, X. F. Liu, J. L. Shen, J. Q. Zhao and G. L. Tu, Synthesis of a Novel Rigid Semi-Alicyclic Dianhydride and Its Copolymerized Transparent Polyimide Films' Properties, *Polymers*, 2022, **14**(19), 12.

16 M. Zhang, W. L. Liu, X. Gao, P. Cui, T. Zou, G. H. Hu, L. M. Tao and L. Zhai, Preparation and Characterization of Semi-Alicyclic Polyimides Containing Trifluoromethyl Groups for Optoelectronic Application, *Polymers*, 2020, **12**(7), 1532.

17 Y. W. Liu, Z. X. Zhou, L. J. Qu, B. Zou, Z. Q. Chen, Y. Zhang, S. W. Liu, Z. G. Chi, X. D. Chen and J. R. Xu, Exceptionally thermostable and soluble aromatic polyimides with special characteristics: intrinsic ultralow dielectric constant, static random access memory behaviors, transparency and fluorescence, *Mater. Chem. Front.*, 2017, **1**(2), 326–337.

18 T. Y. Li, H. H. Huang, L. Wang and Y. M. Chen, High performance polyimides with good solubility and optical transparency formed by the introduction of alkyl and naphthalene groups into diamine monomers, *RSC Adv.*, 2017, **7**(65), 40996–41003.

19 H. T. Zuo, Y. T. Chen, G. T. Qian, F. Yao, H. B. Li, J. Dong, X. Zhao and Q. H. Zhang, Effect of simultaneously introduced bulky pendent group and amide unit on optical transparency and dimensional stability of polyimide film, *Eur. Polym. J.*, 2022, **173**, 111317.

20 K. H. Nam, H. Kim, H. K. Choi, H. Yeo, M. Goh, J. Yu, J. R. Hahn, H. Han, B. C. Ku and N. H. You, Thermomechanical and optical properties of molecularly controlled polyimides derived from ester derivatives, *Polymer*, 2017, **108**, 502–512.

21 L. Yi, C. Y. Li, W. Huang and D. Y. Yan, Soluble polyimides from 4,4'-diaminodiphenyl ether with one or two tert-butyl pedant groups, *Polymer*, 2015, **80**, 67–75.

22 X. H. Huang, M. Mei, C. J. Liu, X. L. Pei and C. Wei, Synthesis and characterization of novel highly soluble and optical transparent polyimides containing tert-butyl and morpholinyl moieties, *J. Polym. Res.*, 2015, **22**(9), 1–9.

23 C. J. Hager, C. D. McMillen, R. Sachdeva, A. W. Martin and J. S. Thrasher, New Fluorine-Containing Diamine Monomers for Potentially Improved Polyimides, *Molecules*, 2023, **28**(19), 15.

24 W. H. Xu, X. R. Ma, Y. H. Su, Y. Song, M. J. Shang, X. M. Lu and Q. H. Lu, Synthesis of highly transparent and thermally stable copolyimide with fluorine-containing dianhydride

and alicyclic dianhydride, *J. Appl. Polym. Sci.*, 2020, **137**(17), 10.

25 X. Z. Huang, F. H. Zhang, Y. J. Liu and J. S. Leng, Flexible and colorless shape memory polyimide films with high visible light transmittance and high transition temperature, *Smart Mater. Struct.*, 2019, **28**(5), 10.

26 C. J. Liu, X. L. Pei, M. Mei, G. Q. Chou, X. H. Huang and C. Wei, Synthesis and characterization of organosoluble, transparent, and hydrophobic fluorinated polyimides derived from 3,3-diisopropyl-4,4-diaminodiphenyl-4-trifluoromethyltoluene, *High Perform. Polym.*, 2016, **28**(10), 1114–1123.

27 A. R. Biery and D. M. Knauss, Synthesis and properties of cationic multiblock polyaramides and polyimides, *J. Polym. Sci.*, 2023, **61**(3), 197–210.

28 H. C. Yu, J. W. Jung, J. Y. Choi, S. Y. Oh and C. M. Chung, Structure-property relationship study of partially aliphatic copolyimides for preparation of flexible and transparent polyimide films, *J. Macromol. Sci., Part A: Pure Appl.Chem.*, 2017, **54**(2), 97–104.

29 S. Dwivedi and T. Kaneko, Molecular Design of Soluble Biopolyimide with High Rigidity, *Polymers*, 2018, **10**(4), 8.

30 X. H. Tong, S. L. Wang, J. N. Dai, S. Wang, X. G. Zhao, D. M. Wang and C. H. Chen, Synthesis and Gas Separation Properties of Aromatic Polyimides Containing Noncoplanar Rigid Sites, *ACS Appl. Polym. Mater.*, 2022, **4**(8), 6265–6275.

31 S. Mehdipour-Ataei, Y. Sarrafi and M. Hatami, Novel thermally stable polyimides based on flexible diamine: synthesis, characterization, and properties, *Eur. Polym. J.*, 2004, **40**(9), 2009–2015.

32 H. J. Ni, X. M. Zhang, J. G. Liu and S. Y. Yang, Intrinsically heat-sealable polyimide films derived from 2,3,3',4'-oxydiphthalic anhydride and aromatic diamines with various ether linkages, *High Perform. Polym.*, 2017, **29**(3), 362–371.

33 Q. Li, H. R. Xiong, L. Pang, Q. H. Li, Y. Zhang, W. Q. Chen, Z. S. Xu and C. F. Yi, Synthesis and characterization of thermally stable, hydrophobic hyperbranched polyimides derived from a novel triamine, *High Perform. Polym.*, 2015, **27**(4), 426–438.

34 Z. Qin, S. Y. Lv, Y. X. Wu, C. Wang, S. Y. Zhang, S. Ban and D. Yin, Synthesis and properties of soluble polyimides containing tert-butyl, ether linkages, and triphenylmethane units, *High Perform. Polym.*, 2020, **32**(8), 924–932.

35 J. H. Chang, Equibiaxially stretchable colorless and transparent polyimides for flexible display substrates, *Rev. Adv. Mater. Sci.*, 2020, **59**(1), 1–9.

36 G. R. Qiu, W. S. Ma and L. Wu, Thermoplastic and low dielectric constants polyimides based on BPADA-BAPP, *Polym.-Plast. Technol. Mater.*, 2020, **59**(13), 1482–1491.

37 X. Wang, H. N. Wang, L. B. Luo, J. Y. Huang, J. Gao and X. Y. Liu, Dependence of pretilt angle on orientation and conformation of side chain with different chemical structure in polyimide film surface, *RSC Adv.*, 2012, **2**(25), 9463–9472.

38 M. Y. Zhang, C. Liu, J. Yang, P. Yang, L. H. Zhang and J. G. Dong, Analysis of the herbicidal mechanism of 4-hydroxy-3-methoxy cinnamic acid ethyl ester using iTRAQ and real-time PCR, *J. Proteomics*, 2017, **159**, 47–53.

39 H. Y. Lei, G. F. Tian, M. F. Xiao, X. L. Li, S. L. Qi and D. Z. Wu, Application of Molecular Simulation in the Study of Polyimide, *Acta Polym. Sin.*, 2019, **50**(12), 1253–1262.

40 P. C. Tan, B. S. Ooi, A. L. Ahmad and S. C. Low, Monomer atomic configuration as key feature in governing the gas transport behaviors of polyimide membrane, *J. Appl. Polym. Sci.*, 2018, **135**(14), 11.

41 R. Swaidan, B. Ghanem, E. Litwiller and I. Pinnau, Effects of hydroxyl-functionalization and sub-Tg thermal annealing on high pressure pure- and mixed-gas CO2/CH4 separation by polyimide membranes based on 6FDA and triptycene-containing dianhydrides, *J. Membr. Sci.*, 2015, **475**, 571–581.

42 H. Y. Lei, F. Bao, W. F. Peng, L. H. Qiu, B. Y. Zou and M. J. Huang, Torsion effect of the imide ring on the performance of transparent polyimide films with methyl-substituted phenylenediamine, *Polym. Chem.*, 2022, **13**(48), 6606–6613.

43 C. H. Yi, W. M. Li, S. Shi, K. He, P. C. Ma, M. Chen and C. L. Yang, High-temperature-resistant and colorless polyimide: Preparations, properties, and applications, *Sol. Energy*, 2020, **195**, 340–354.

44 L. L. Chen, H. Yu, M. Dirican, D. J. Fang, Y. Tian, C. Y. Yan, J. Y. Xie, D. M. Jia, H. Liu, J. S. Wang, F. C. Tang, X. W. Zhang and J. S. Tao, Highly Transparent and Colorless Nanocellulose/Polyimide Substrates with Enhanced Thermal and Mechanical Properties for Flexible OLED Displays, *Adv. Mater. Interfaces*, 2020, 7(20), 11.

45 F. Bao, L. H. Qiu, B. Y. Zou, H. Y. Lei, W. F. Peng, S. Z. D. Cheng and M. J. Huang, Development of Fluorinated Colorless Polyimides of Restricted Dihedral Rotation toward Flexible Substrates with Thermal Robustness, *Macromolecules*, 2024, **57**(8), 3568–3579.

46 Y. Z. Fang, X. J. He, J. C. Kang, L. Wang, T. M. Ding, X. M. Lu, S. Y. Zhang and Q. H. Lu, Colorless transparent and thermally stable terphenyl polyimides with various small side groups for substrate application, *Eur. Polym. J.*, 2024, **202**, 112640.

47 H. Y. Lei, X. L. Li, J. L. Wang, Y. H. Song, G. F. Tian, M. J. Huang and D. Z. Wu, DFT and molecular dynamic simulation for the dielectric property analysis of polyimides, *Chem. Phys. Lett.*, 2022, **786**, 139131.

48 P. K. Tapaswi, M. C. Choi, K. M. Jeong, S. Ando and C. S. Ha, Transparent Aromatic Polyimides Derived from Thiophenyl-Substituted Benzidines with High Refractive Index and Small Birefringence, *Macromolecules*, 2015, **48**(11), 3462–3474.

49 X. W. Peng, W. H. Xu, L. L. Chen, Y. C. Ding, T. R. Xiong, S. L. Chen and H. Q. Hou, Development of high dielectric polyimides containing bipyridine units for polymer film capacitor, *React. Funct. Polym.*, 2016, **106**, 93–98.

50 T. W. Zhu, Q. X. Yu, W. W. Zheng, R. X. Bei, W. H. Wang, M. M. Wu, S. W. Liu, Z. G. Chi, Y. Zhang and J. R. Xu, Intrinsic high-k-low-loss dielectric polyimides containing ortho-position aromatic nitrile moieties: reconsideration on Clausius-Mossotti equation, *Polym. Chem.*, 2021, **12**(16), 2481–2489.